

Combination of aN³LO PDFs and implications for Higgs production cross-sections at the LHC

The MSHT Collaboration:

Thomas Cridge¹, Lucian A. Harland-Lang², Jamie McGowan², and Robert S. Thorne²

The NNPDF Collaboration:

Richard D. Ball³, Alessandro Candido⁴, Stefano Carrazza⁵, Juan Cruz-Martinez⁴, Luigi Del Debbio³,
Stefano Forte⁵, Felix Hekhorn^{6,7}, Giacomo Magni^{8,9}, Emanuele R. Nocera¹⁰,
Tanjona R. Rabemananjara^{8,9}, Juan Rojo^{8,9}, Roy Stegeman³, and Maria Ubiali¹¹

¹ *Deutsches Elektronen-Synchrotron DESY, Notkestr. 85, 22607 Hamburg, Germany*

² *Department of Physics and Astronomy, University College London, London, WC1E 6BT, UK*

³ *The Higgs Centre for Theoretical Physics, University of Edinburgh,
JCMB, KB, Mayfield Rd, Edinburgh EH9 3FD, Scotland*

⁴ *CERN, Theoretical Physics Department, CH-1211 Geneva 23, Switzerland*

⁵ *Tif Lab, Dipartimento di Fisica, Università di Milano and
INFN, Sezione di Milano, Via Celoria 16, I-20133 Milano, Italy*

⁶ *University of Jyväskylä, Department of Physics, P.O. Box 35, FI-40014 University of Jyväskylä, Finland*

⁷ *Helsinki Institute of Physics, P.O. Box 64, FI-00014 University of Helsinki, Finland*

⁸ *Department of Physics and Astronomy, Vrije Universiteit, NL-1081 HV Amsterdam*

⁹ *Nikhef Theory Group, Science Park 105, 1098 XG Amsterdam, The Netherlands*

¹⁰ *Dipartimento di Fisica, Università degli Studi di Torino and
INFN, Sezione di Torino, Via Pietro Giuria 1, I-10125 Torino, Italy*

¹¹ *DAMTP, University of Cambridge, Wilberforce Road, Cambridge, CB3 0WA, United Kingdom*

Abstract

We discuss how the two existing approximate N³LO (aN³LO) sets of parton distributions (PDFs) from the MSHT20 and NNPDF4.0 series can be combined for LHC phenomenology, both in the pure QCD case and for the QCD⊗QED sets that include the photon PDF. Using the resulting combinations, we present predictions for the total inclusive cross-section for Higgs production in gluon fusion, vector boson fusion, and associated production at the LHC Run-3. For the gluon fusion and vector boson fusion channels, the corrections that arise when using correctly matched aN³LO PDFs with N³LO cross section calculations, compared to using NNLO PDFs, are significant, in many cases larger than the PDF uncertainty, and generally larger than the differences between the two aN³LO PDF sets entering the combination. The combined aN³LO PDF sets, MSHT20xNNPDF40_an3lo and MSHT20xNNPDF40_an3lo_qed, are made publicly available in the LHAPDF format and can be readily used for LHC phenomenology.

1 Introduction

The two global determinations of parton distribution functions (PDFs) from the MSHT [1] and NNPDF [2] collaborations have been recently extended to approximate next-to-next-to-next-to-leading order (aN³LO), in Refs. [3] and [4] respectively. Both the MSHT and NNPDF aN³LO PDF sets have been subsequently enlarged to also include a photon PDF and mixed QED⊗QCD corrections to perturbative evolution [5, 6].

The inclusion of N³LO QCD corrections in the determination of these PDF sets is approximate in two different respects. First, N³LO perturbative evolution is only known approximately. Indeed, splitting functions are not known exactly, so an approximation to them must be constructed based on exact knowledge of their small- and large- x behavior and a finite set of Mellin moments [7–17]. Knowledge of N³LO splitting functions has progressed rapidly, with more Mellin moments being gradually published over the years. In fact, now [18, 19] the full set of Mellin moments up to $N = 20$ is available for all elements of the splitting function matrix. Heavy quark transition matrix elements at $\mathcal{O}(\alpha_s^3)$, which are needed for massless perturbative evolution in a variable-flavor number scheme, are now also fully known, albeit only recently in complete form [20–30]. Hence N³LO perturbative evolution is known exactly for all practical purposes, as we shall discuss in somewhat more detail below.

Second, however, N³LO partonic cross-sections are known only for massless deep-inelastic scattering (DIS) [31] and for the total Drell-Yan cross-section and on-shell rapidity distribution [32–36], which are a subset of the processes used for PDF determination. In particular, whereas the computation of the high Q^2 limit of heavy quark structure functions was recently completed, permitting the determination of heavy quark transition matrix elements, the computation of corrections to DIS coefficient functions proportional to powers of $\frac{m_h^2}{Q^2}$ of the heavy quark mass is beyond the current state of the art, as is the computation of fiducial N³LO corrections to hadronic processes, which are needed for a meaningful comparison to hadron collider data.

As a consequence, while approximate N³LO perturbative evolution is close to exact, knowledge of N³LO hard cross sections is limited. Moreover, massless DIS data do not fully determine the PDFs, and consequently a N³LO PDF determination must include a number of processes for which only NNLO matrix elements are available. It is in this respect that perturbative accuracy in aN³LO PDF determination is not fully N³LO.

The two available aN³LO PDF determinations include estimates of the uncertainty due to incomplete knowledge of N³LO terms, namely, both the incomplete knowledge of splitting functions, and the missing N³LO hard cross-sections, as well as that related to missing perturbative corrections at N⁴LO and beyond. In Ref. [3] (MSHT) the uncertainty estimation is done by means of nuisance parameters, while in Ref. [4] (NNPDF) it is done through a theory covariance matrix. As is well known, (see e.g. Refs. [37, 38]) the nuisance parameter and theory covariance matrix approaches are completely equivalent for Gaussian uncertainties, provided only the eigenvectors and eigenvalues of the covariance matrix coincide with the nuisance parameters and their uncertainties.

The approaches of Refs. [3, 4] consequently only differ in the way the covariance matrix, or the corresponding nuisance parameters, are estimated. In Ref. [3] this is done based on a judicious estimate of the form of missing terms, which also incorporates effects of varying the parametrization of the splitting functions. In Ref. [4], instead, the contributions to the covariance matrix due to incomplete knowledge of splitting functions are estimated differently from all those due to missing higher order terms (missing N⁴LO splitting functions, missing N⁴LO massless DIS coefficient function, and missing N³LO hard cross sections for all other processes). Namely, variation of the parametrization of splitting functions (as in Ref. [3]) is used for the estimate of their incomplete knowledge, while renormalization and factorization scale variation is used for missing higher order perturbative corrections.

Both Refs. [3, 4] included all the information that was available at the time of their publication, and consequently, because Ref. [3] was published earlier, it included less information on N³LO evolution, and specifically it did not yet include the more recent information on Mellin moments from Refs. [11, 14–16, 39], and the exact knowledge of the heavy quark transition matrix elements, both of which are instead included in Ref. [4] (with the only exception of the heavy quark terms of Ref. [30]) as they had become available meanwhile. Neither determination includes the higher moments of P_{gq} [17] and P_{gg} [18, 19]. Some uncertainties in Ref. [3] are accordingly larger, but with the information now available it is possible to check that uncertainties in Refs. [3, 4] were estimated accurately.

Specifically, the uncertainty on splitting functions with Mellin moments up to $N = 20$ for all matrix

elements but P_{gg} was assessed in both Refs. [4, 16] with very similar results, and shown in Ref. [4] to be smaller than the uncertainty due to the missing N⁴LO corrections estimated by scale variation. This assessment was extended to P_{gg} recently in Ref. [19]. The only other uncertainty on perturbative evolution present in Ref. [4] are the contributions, computed in Ref. [30], to transition matrix elements, which however were found in Ref. [30] to agree perfectly within the uncertainty band with the previous approximation [20] adopted in Ref. [4]. Based on this, it can be safely concluded that, as mentioned, N³LO perturbative evolution is fully known for all practical purposes. Furthermore, the splitting functions of Refs. [3, 4] agree within uncertainties, with the exception of the P_{gq} splitting function, that differs at approximately the two-sigma level, see also the benchmarking comparison of [40, 41]. Note, however, that as far as PDF evolution is concerned P_{gg} is much more important than P_{gq} , and the effects at small- x are to a large extent anti-correlated. Updated knowledge of the splitting functions effectively removes this one source of moderate discrepancy. A preliminary analysis of the effect of including these additional Mellin moments, and hence improved splitting functions, which have been determined since the original MSHT publication was presented in [42], and observed a small increase in the gluon near $x = 0.01$, though still within the original MSHT uncertainties. While this is significantly washed out in parton luminosities, it does further improve the agreement between the two PDF sets.

Estimates of the impact of the use of aN³LO PDFs in the computation of the Higgs total production cross-section in both Refs. [3, 4] suggest that using NNLO PDFs, instead of aN³LO PDFs, with the N³LO matrix element for Higgs production in gluon fusion and vector boson fusion leads to an error that is comparable to, or even larger than the PDF uncertainty on the N³LO result. Also, this error is found [4] to be rather larger than the estimate of its size [43, 44] based on the corresponding shift at one less perturbative order. This suggests that using NNLO PDFs in the N³LO computation spoils the accuracy of the N³LO result, in a way that, moreover, may not be reflected in a corresponding increase in uncertainty, if the latter is estimated in this way.

Given the availability of two different aN³LO PDF sets, accurate N³LO phenomenology requires therefore a comparison of the impact of the use of either of these PDF sets, and a prescription for their combination. It is the purpose of this brief note to provide a first assessment and suggest a possible prescription, having specifically in view Higgs production in gluon fusion, but presenting results also for other Higgs production modes. We will first compare the aN³LO PDFs of Refs. [3, 4], both without and with QED corrections, to each other, then assess for each of them the impact of aN³LO corrections on parton luminosities, and finally construct a combination of these PDFs based on PDF4LHC combination methodology [45]. We will finally discuss results for the cross-section for Higgs production in gluon fusion and other channels based on individual and combined aN³LO PDF sets.

2 Comparison of aN³LO PDFs

We first compare the NNPDF4.0 and MSHT20 aN³LO PDF sets both with and without QED effects.

When comparing MSHT and NNPDF PDF sets, care must be taken to compare sets that include the same uncertainties. Specifically, all NNPDF4.0 PDF sets are now delivered in two different versions, one in which the PDF uncertainty includes the uncertainty due to missing higher-order corrections on the theory predictions used for PDF determination (MHOU, henceforth), and the other in which it does not. Hence uncertainties due to missing N⁴LO corrections are only included by NNPDF in the aN³LO MHOU sets, though both NNPDF and MSHT aN³LO sets include uncertainties due to missing N³LO corrections to hadronic processes and massive DIS. Note that the NLO and NNLO sets with MHOU were not included at the time of first release of NNPDF4.0 [2], and only released at a later stage [46]. On the other hand, in the MSHT approach all uncertainties, including all MHOUs, are included at N³LO, while MHOUs are not included at NNLO (as they were not in the original NNLO NNPDF4.0 PDFs of Ref. [2]). The pertinent comparison of the MSHT20 sets is therefore at N³LO with the NNPDF4.0 sets with MHOUs included, while at NNLO with the NNPDF4.0 sets without MHOUs. Note that in Ref. [4] the MSHT20 aN³LO PDFs were instead compared to the NNPDF4.0 set without MHOUs. Henceforth we will here tacitly assume that for NNPDF4.0 NNLO refers to the non-MHOU sets while aN³LO refers to the MHOU sets.

When comparing the aN³LO PDF sets, it should of course be borne in mind that the MSHT20 and NNPDF4.0 sets already differ at NNLO due to differences in dataset and methodology. On top of the difference in basic underlying methodology, namely generalized polynomial parametrization and Hessian uncertainties for MSHT, neural network parametrization and Monte Carlo uncertainties for NNPDF, several

details of the theoretical approach also differ. Specifically, there are several differences in the treatment of heavy quarks: the values of heavy quark masses are somewhat different; the charm PDF is fitted to the data in NNPDF4.0, while in MSHT20 it is determined by perturbative matching conditions; and for DIS the massive and massless heavy quark schemes are matched using the Thorne-Roberts scheme by MSHT and the FONLL scheme by NNPDF. A detailed comparison of the NNLO MSHT20 and NNPDF4.0 PDF sets was performed in Ref. [2], see in particular Fig. 21 and Fig. 60 of that reference. Several of the differences seen in the comparison of Ref. [2] are also seen when comparing MSHT20 to the previous NNPDF3.1 PDF set, and indeed many of the methodological differences (in particular those related to the treatment of heavy quarks) are the same. This is relevant because MSHT20 and NNPDF3.1 were included in a detailed benchmarking presented in Ref. [47, 48], along with the CT18 PDF set. In this work, "reduced" PDF sets from the three groups were produced by adopting common assumptions and settings (specifically for the treatment of heavy quarks), instead of the inconsistent settings used in the original fits. The reduced sets turned out to be in quite good agreement with each other within uncertainties, thereby showing that the differences between the original sets were due to these inconsistent settings.

These more consistent reduced sets were then used to produce the PDF4LHC21 combination [47]. The combination that we will discuss here is instead based on the publicly available aN³LO PDF sets, thereby leading to a more conservative uncertainty estimate that encompasses the differences between the PDF sets entering the combination, as we shall explain below. To understand the features of this combination we therefore start with a comparison of the published MSHT20 and NNPDF4.0 aN³LO sets, along with the NNLO sets, to see how much of the differences seen at aN³LO reflect those already present at NNLO, whose origin was largely understood in Refs. [47, 48].

The comparison of the aN³LO sets is presented in Figs. 1-2 (left), together with the comparison of the corresponding NNLO sets (right). The aN³LO sets including QED corrections are compared in Fig. 3. All PDFs are shown at $Q = 100$ GeV, normalized to the NNPDF4.0 central value. All error bands are one sigma uncertainties. The dominant differences between the aN³LO PDF sets are essentially the same as at NNLO, with the largest difference observed for the charm PDF, which, as mentioned, is independently parametrized in NNPDF4.0, but not in MSHT20, where it is determined by perturbative matching conditions. Indeed, it is clear from Figs. 1-2 that most differences between MSHT and NNPDF change very little when moving from NNLO to aN³LO. An exception is the gluon PDF, which differs more between NNPDF and MSHT at aN³LO. Specifically, while reasonably compatible for $x \lesssim 0.07$ at NNLO, the MSHT and NNPDF gluons disagree at aN³LO, with the MSHT20 result suppressed in comparison to NNPDF4.0 by 3-4% in the region $10^{-3} \lesssim x \lesssim 10^{-1}$, with a PDF uncertainty of 1-2%.

This suppression can, to some extent, be traced to the difference in the behavior of P_{gq} mentioned in the introduction. The P_{gq} splitting function contains more unknown small- x divergent terms than the other splitting functions, and hence has more potential uncertainty at small x , especially if a color-charge relationship that would relate these unknown terms to known contributions to P_{gg} is not assumed to be approximately true for subleading terms (and indeed it is assumed by NNPDF but not by MSHT). Hence, with the smaller moment information and weaker constraints used by MSHT [3], deviations are possible but have been largely eliminated with the improved information now available.

In practice, the differences between the two aN³LO PDF sets are at most at the two sigma level. Furthermore, a recent MSHT preliminary study shows that updating the splitting function with the additional moments now known [14–16] results in a $\sim 1.5\%$ increase in the gluon at $x \sim 0.01$ [42], though it does still remain within the uncertainty band of the original MSHT determination, thereby further reducing differences. Hence, updates in P_{gq} do improve the comparison, but do not remove the difference in the gluon. Recall however that, as mentioned in Sect. 1, the very recent additional moments now known for P_{gq} [17] and P_{gg} [18, 19] are not included in either the MSHT or NNPDF sets discussed here. Finally, the inclusion of the photon PDF also has a moderate impact on the other PDFs, mostly limited to a suppression of the gluon PDF due to the 1% shift in momentum fraction from the gluon to the photon, as well as some reduction in the u, \bar{u} PDFs at high x , due to $q \rightarrow q\gamma$ splitting.

The MSHT and NNPDF aN³LO parton luminosities are compared in Figs. 4-5, respectively without and with QED effects, while, in order to appreciate better the impact of N³LO corrections, the aN³LO luminosities are compared for each set to the respective NNLO luminosities in Fig. 6, normalized to the aN³LO result. The pattern of differences reproduces that seen at the level of PDFs, with a suppression of the MSHT gluon-gluon, quark-antiquark, and gluon-quark luminosities in comparison to NNPDF in the $M_X \sim 100$ GeV region, while the quark-quark luminosity in the two sets is very similar. The suppression can be traced to the behavior of the light quark and gluon PDFs seen in Figs. 1-2 (right). Interestingly, the

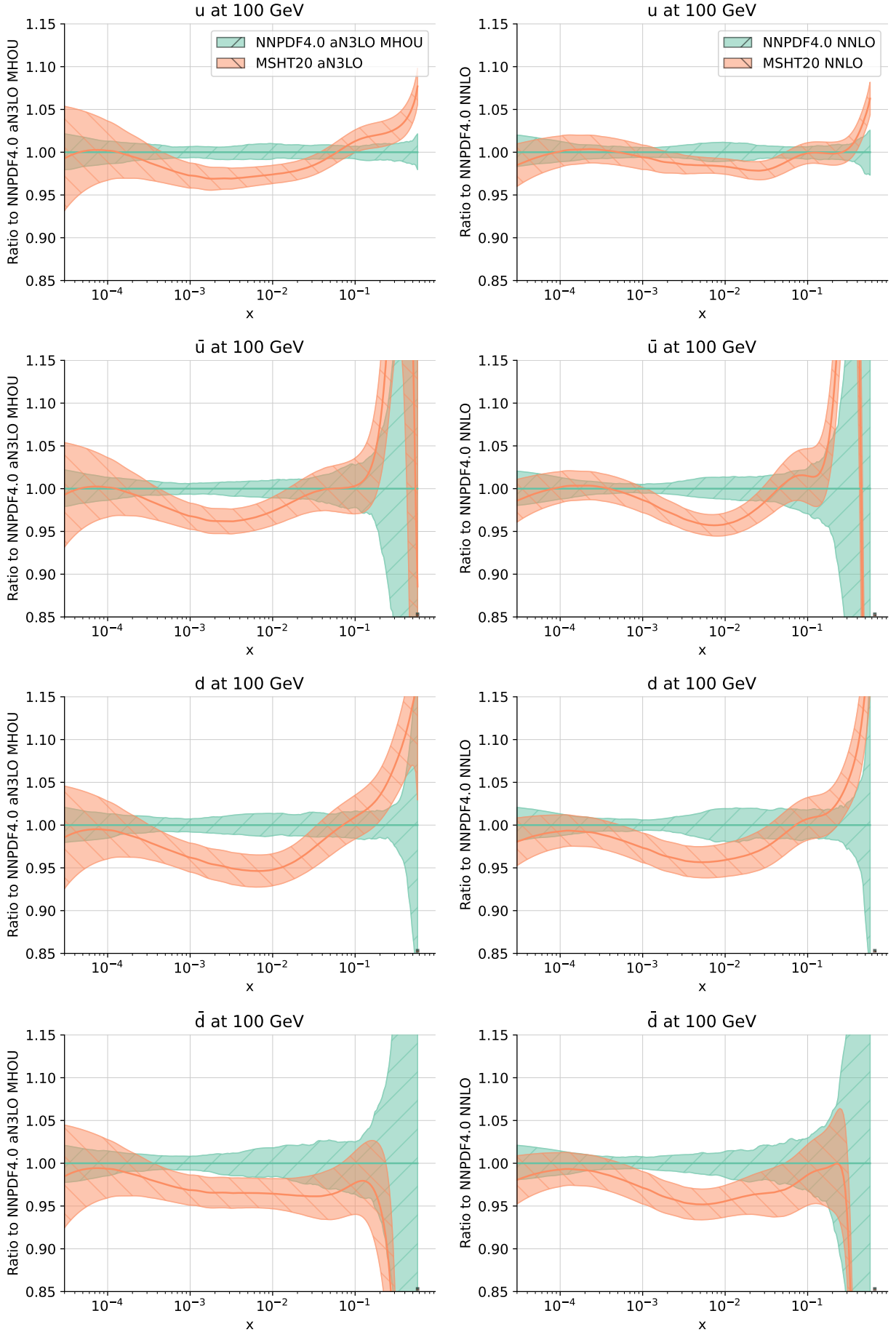


Figure 1. The NNPDF4.0 and MSHT20 aN³LO (left) and NNLO (right) PDFs, for the u and d sector at $Q = 100$ GeV, shown as a ratio to NNPDF4.0. All uncertainties shown are one sigma.

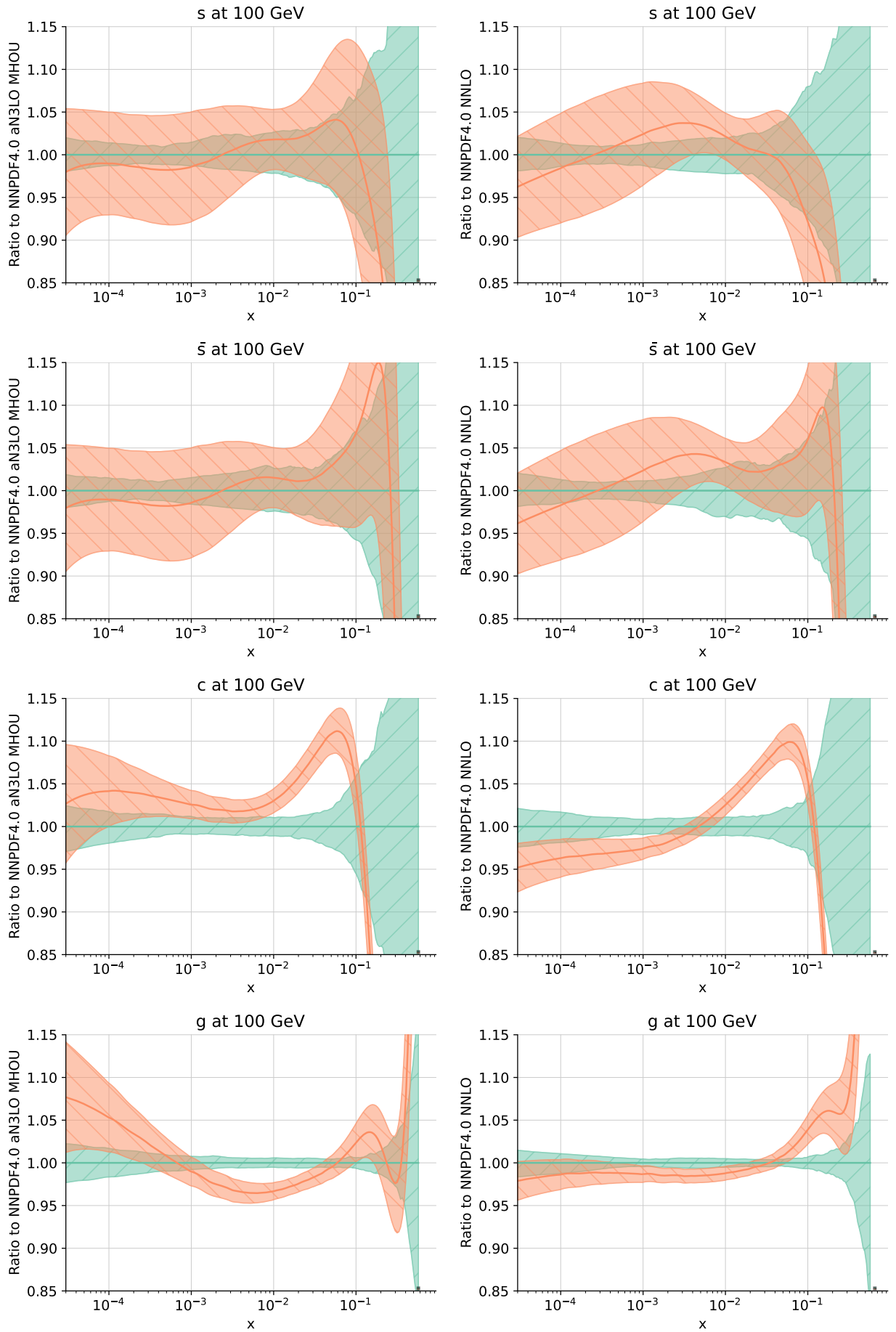


Figure 2. As in Fig. 1 but for the s, \bar{s}, c, g PDFs.

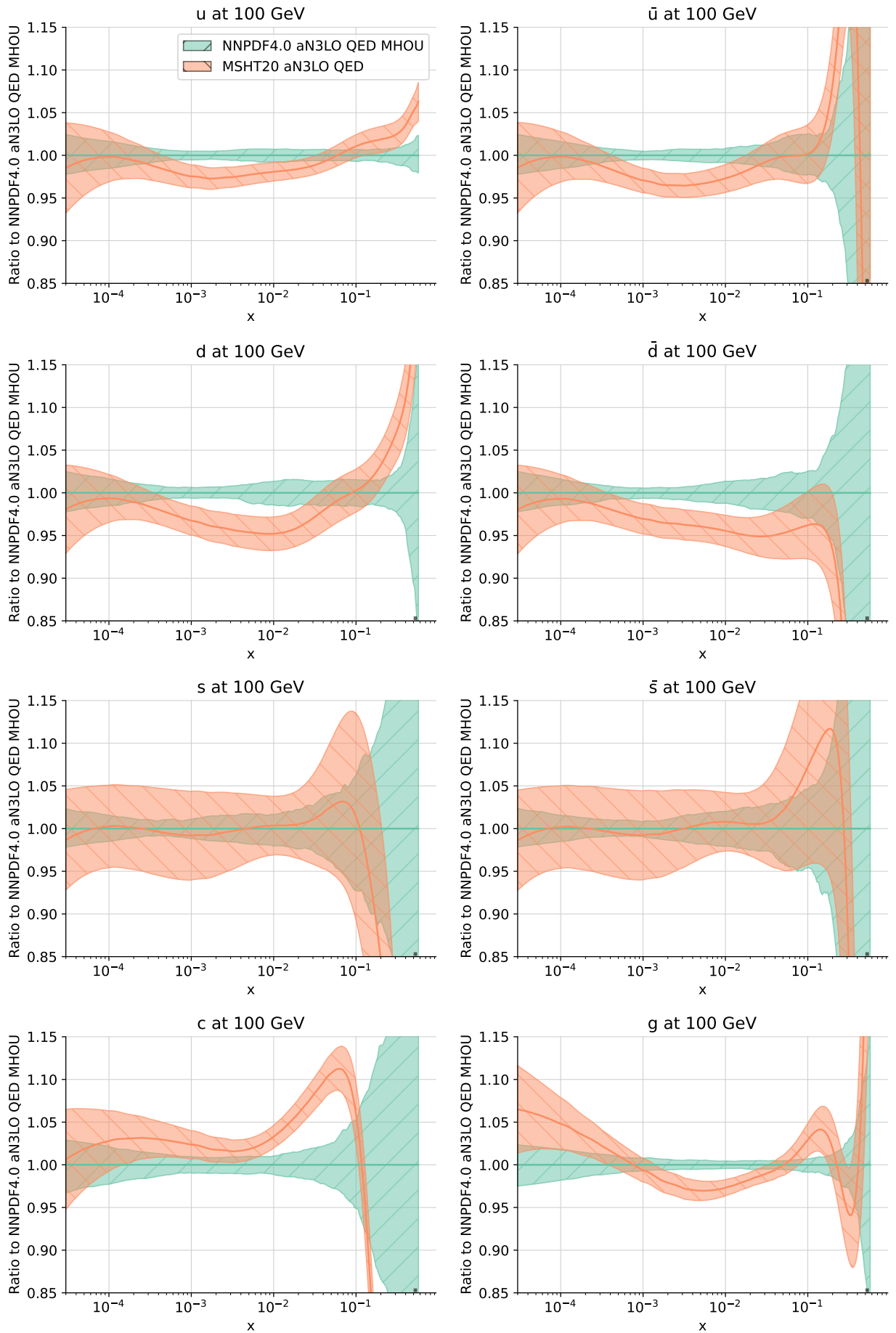


Figure 3. The NNPDF4.0 MHOUs and MSHT20 aN³LO + QED PDFs at $Q = 100$ GeV, shown as a ratio to NNPDF4.0. All uncertainties shown are one sigma.

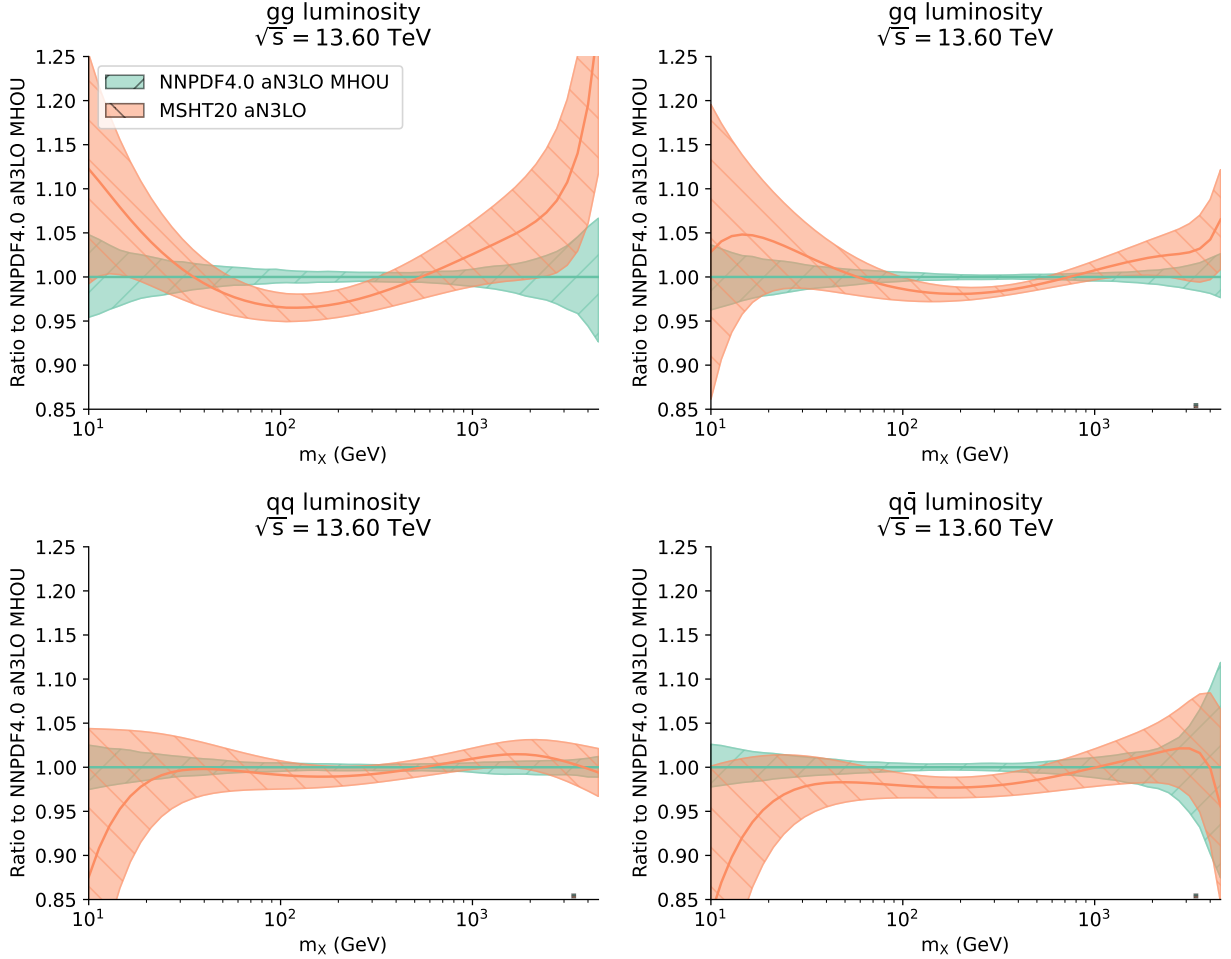


Figure 4. The same comparison as in Figs. 1-2 (right) but for the corresponding parton luminosities.

difference in gluon-gluon luminosity is slightly reduced for the QED PDF sets compared to the pure QCD sets.

The qualitative impact of the aN³LO corrections on either set for $M_X \gtrsim 30$ GeV is similar (and almost identical for the quark-quark luminosity), but with a stronger aN³LO suppression of gluon luminosities for MSHT20. In particular the gluon-gluon luminosity is suppressed for $10^2 \lesssim m_X \lesssim 10^3$ GeV by about 3% in NNPDF4.0 and up to 6% in MSHT20 and the gluon-quark luminosity is suppressed in the same region by about 1% in NNPDF4.0 and 3% in MSHT20. Note that the impact on this comparison of the aforementioned update studied in Ref. [42] of the splitting functions in MSHT is very small due to the integration over rapidity washing out small differences in the gluon.

These comparisons show that the differences between NNLO and aN³LO for each set are generally larger than the differences between the two aN³LO sets, or indeed the two NNLO sets, especially in the case of MSHT. Furthermore, the differences between NNLO and aN³LO PDFs are often comparable and sometimes (specifically for the gluon-gluon luminosity) larger than the respective PDF uncertainties. These two observations taken together suggest that the use of aN³LO PDFs is mandatory for accurate N³LO phenomenology, because using NNLO PDFs with the aN³LO matrix element leads to an error that may be larger than the PDF uncertainty, especially in the Higgs gluon and vector boson fusion channels, that are respectively mostly sensitive to the gluon-gluon and quark-quark luminosities. Therefore, even though the MSHT and NNPDF aN³LO PDF sets do not always agree within uncertainties, their combination will lead to results that are more accurate than the use of NNLO PDFs. These considerations motivate the construction of a combined aN³LO PDF set.

3 Combination of aN³LO PDFs

Based on the PDF comparisons presented in Sect. 2, phenomenological predictions for hadronic processes at N³LO could be obtained by simply using the two available aN³LO PDF sets and combining results as

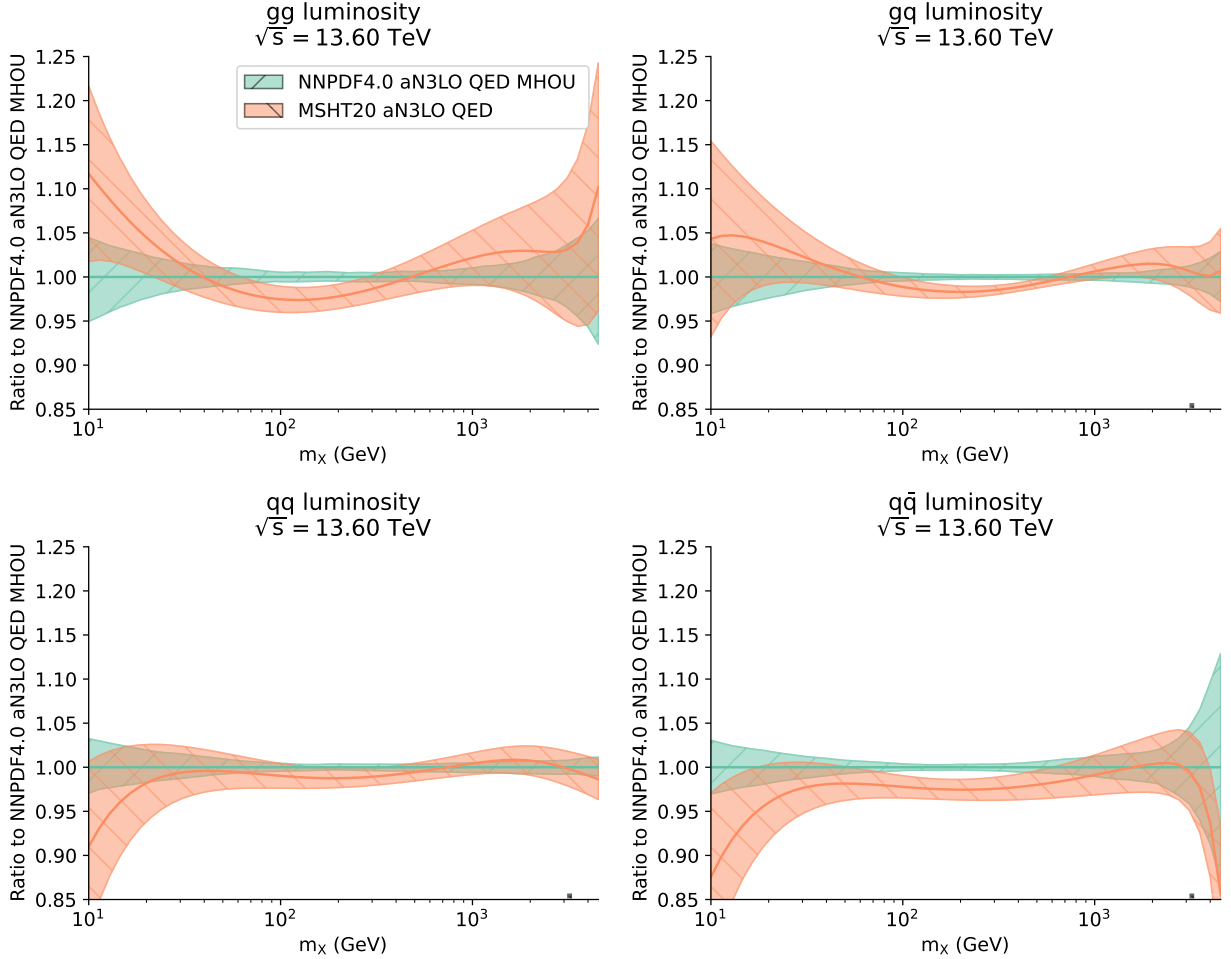


Figure 5. The same comparison as in Fig. 4 but including QED corrections.

a weighted average. However, given that the two sets do not always agree within uncertainties, a more conservative way of estimating the uncertainty on the final result is advisable, such as the so-called PDG prescription and variations thereof [49], see also Sect. 12.5 of Ref. [50].

An effective way of arriving at a conservative uncertainty estimate in our case is to produce unweighted Monte Carlo combined PDF sets [45, 51]. This is done by first turning all the PDF sets to be combined into a set of Monte Carlo replicas, which for Hessian sets can be done using the methodology of Ref. [52], and then merging an equal number of replicas from each set into a single replica set. The merged set then corresponds to a probability distribution that is the equally likely combination of the probability distribution of the input sets, and thus will lead to uncertainties that encompass those of the sets that are being combined.

We have produced this combination by merging 100 Monte Carlo replicas produced using the method of Ref. [52] from the default Hessian aN³LO set of Ref. [1] after symmetrization of the Hessian uncertainties, with 100 replicas from the MHO set of Ref. [46]. In order to improve numerical stability of results, for the NNPDF4.0 PDFs the (x, Q^2) interpolation LHAPDF grid has been recast to match the MSHT20 grid. We have then repeated the procedure for the QED variants presented in Refs. [5, 6]. We will henceforth denote these combined PDF sets as MSHT20xNNPDF40_aN3LO; the corresponding LHAPDF grid files are MSHT20xNNPDF40_an3lo and MSHT20xNNPDF40_an3lo_qed. We have also produced combined pure QCD and QCD⊗QED NNLO sets obtained using the same procedure, but now starting from the NNPDF4.0 and MSHT NNLO PDF sets. The sole purpose of these sets is to provide a baseline to the corresponding aN³LO sets, in order to assess the effect of N³LO corrections with everything else unchanged. In particular, they should not be viewed as a substitute for the PDF4LHC21 NNLO combined sets. These sets are denoted as MSHT20xNNPDF40_NNLO, and the corresponding LHAPDF grid files MSHT20xNNPDF40_nn1o and MSHT20xNNPDF40_nn1o_qed. Note that, as discussed in Sect. 2, the aN³LO sets do include while the NNLO sets do not include uncertainties due to MHO in the theory predictions used for PDF determination.

It should always be kept in mind that, as already mentioned, unlike the PDF4LHC21 combined PDFs [47], these aN³LO and NNLO MSHT20xNNPDF40 PDFs are an unmodified combination of the two input sets,

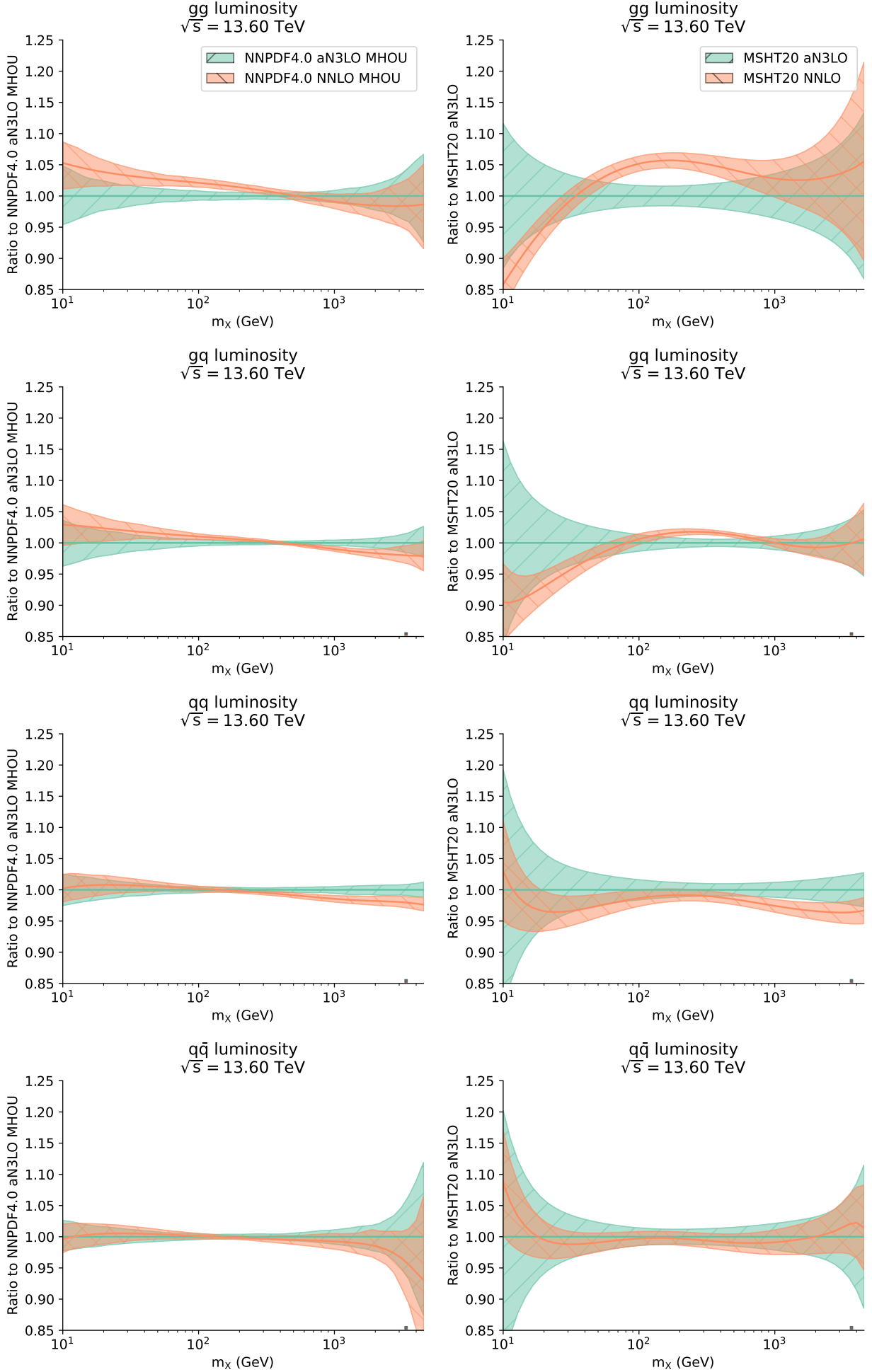


Figure 6. Comparison of NNLO and aN³LO parton luminosities for NNPDF4.0 (left) and MSHT20 (right), normalized to the aN³LO result.

which are based on somewhat different theoretical and methodological assumptions. They should be viewed as a means to obtain accurate but conservative N³LO predictions for LHC processes, not as an optimized PDF combined set. For example, due to the aforementioned different treatment of heavy quarks, the combined PDFs are only reliable for scales well above the heavy quark thresholds, and should not be used in regions where heavy quark mass effects are relevant, such as Higgs production via bottom quark fusion. However, we will show below that for scales $M_X \gtrsim 50$ GeV the effects of these different treatments of quark masses are in general smaller than the differences between NNLO vs. aN³LO PDFs.

The combined aN³LO PDFs are displayed at $Q = 100$ GeV in Figs. 7-8, respectively without and with QED effects, together with the two sets that are being merged, shown as a ratio to the central value of the combined set. The central value of the combined set is, by construction, the unweighted average of the two starting sets, and the uncertainty is seen to encompass that of the two sets that enter the combination.

In order to assess the impact of the N³LO corrections, in Fig. 9 we compare luminosities for the LHC $\sqrt{s} = 13.6$ TeV at NNLO and aN³LO, in the latter case both without and then with QED corrections, shown as a ratio to the NNLO result, computed using the PDF4LHC21 combined NNLO PDF set [47]. For reference, the NNLO sets are compared to each other in Fig. 10, where we show the two different combinations, PDF4LHC21 and MSHT20xNNPDF40_NNLO, the latter both without and with QED corrections. It is clear that for the gluon-gluon and quark-quark luminosities at all scales $M_X \gtrsim 100$ GeV the impact of the aN³LO corrections is quite significant and in the gluon-gluon channel well outside the NNLO uncertainty band. On the other hand, the difference between the two NNLO combinations is significantly smaller, with each of them well within the uncertainty band of the other, thereby showing that the significance of the aN³LO does not depend on the NNLO baseline that one compares it to. For the gluon-gluon luminosity the impact of QED corrections is also significant, both at NNLO and aN³LO.

It is interesting to observe that for the gluon-gluon luminosity in the range $30 \lesssim M_X \lesssim 300$ GeV the difference between aN³LO and NNLO is significantly larger than the difference between NNLO and NLO, with the effect peaking around $M_X \sim 100$ GeV (see Fig. 24 of Ref. [4]), though somewhat reduced upon the inclusion of MHOUs. This can be understood as the consequence of the fact that at N³LO there is a leading small x logarithmic contribution to P_{gg} and P_{gq} , which instead accidentally vanishes both at NLO and NNLO. This results in N³LO corrections leading to sizable contribution to gluon evolution even at intermediate x : indeed, both splitting functions at N³LO are qualitatively similar to the form that one obtains when including into the splitting function full small- x resummation [4]. Furthermore, the effect of N³LO corrections on splitting functions, heavy flavour contributions, and light quark coefficient functions all conspire to push the gluon in the same direction for all $x \lesssim 0.1$ (see Fig. 44 of Ref. [3]).

4 Implications for Higgs production

We now present predictions for Higgs production at the LHC in gluon fusion, in vector boson fusion (VBF), and in association with a weak gauge boson (hV). Results are collected in Tables 1-2 and displayed in Fig. 11. All results shown are computed for the LHC with $\sqrt{s} = 13.6$ TeV using N³LO matrix elements, and only differ in the input PDF set. No QED or electroweak corrections are included in the matrix element, and in particular photon-initiated processes are not included, although for e.g. associated hW^\pm production these enter at the percent level, see e.g. [53].

The cross-sections are computed using the `ggHiggs` code [44] for gluon fusion, `n3lox`s [43] for associated production, and `proVBFH` [54, 55] for vector boson fusion. The central factorization and renormalization scales are set to $\mu_F = \mu_R = m_H/2$ for Higgs production in gluon fusion, $\mu_F = \mu_R = Q_V$ (the vector boson virtuality) for VBF, and $\mu_F = \mu_R = m_{hV}$, the event-by-event invariant mass of the hV system, in associated production. In Fig. 11 we do not display the hW^- cross-sections since they have the same qualitative behavior as the hW^+ cross-sections, as can also be observed from Table 1.

The uncertainties shown in Tables 1-2 and in Fig. 11 are the pure PDF uncertainty (first uncertainty in the table and inner error bar in the figure) as well as the sum in quadrature of the PDF uncertainty and MHO uncertainties on the matrix element, the latter evaluated with the 7 point scale variation prescription (second uncertainty in the table and outer error bar in the figure). For the VBF and hV production channels the two uncertainties essentially coincide, because scale variations are negligible and the PDF uncertainty dominates, while in the gluon-fusion cross-sections scale errors represent the largest theoretical uncertainty.

Results are shown for the MSHT20 and NNPDF4.0 aN³LO sets both with and without QED corrections, and the combined MSHT20xNNPDF40 aN³LO sets constructed here, also with and without QED

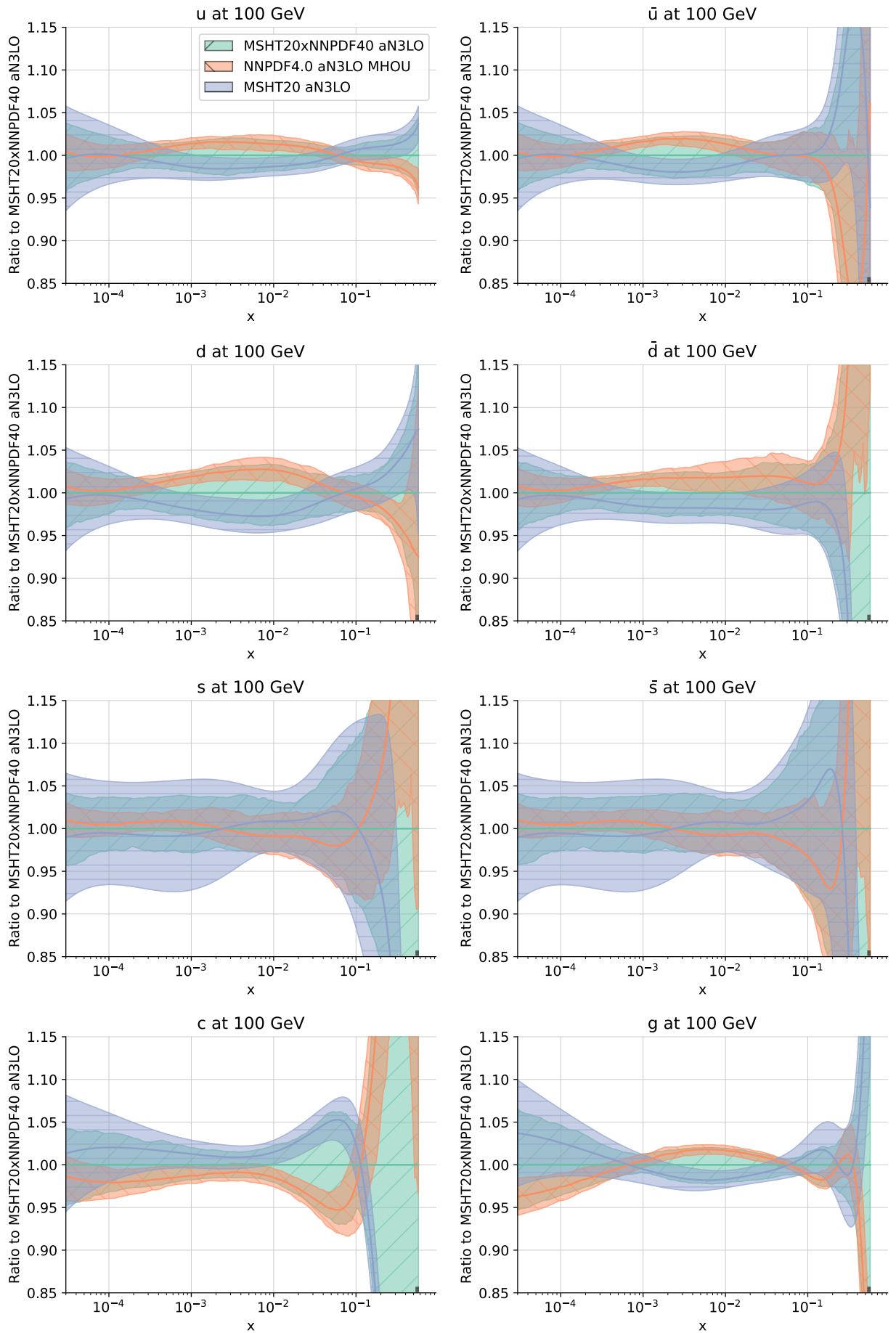


Figure 7. The combined MSHT20xNNPDF40_aN3LO PDFs, compared to the NNPDF and MSHT aN³LO PDFs that enter the combination, shown as a ratio to MSHT20xNNPDF40_aN3LO.

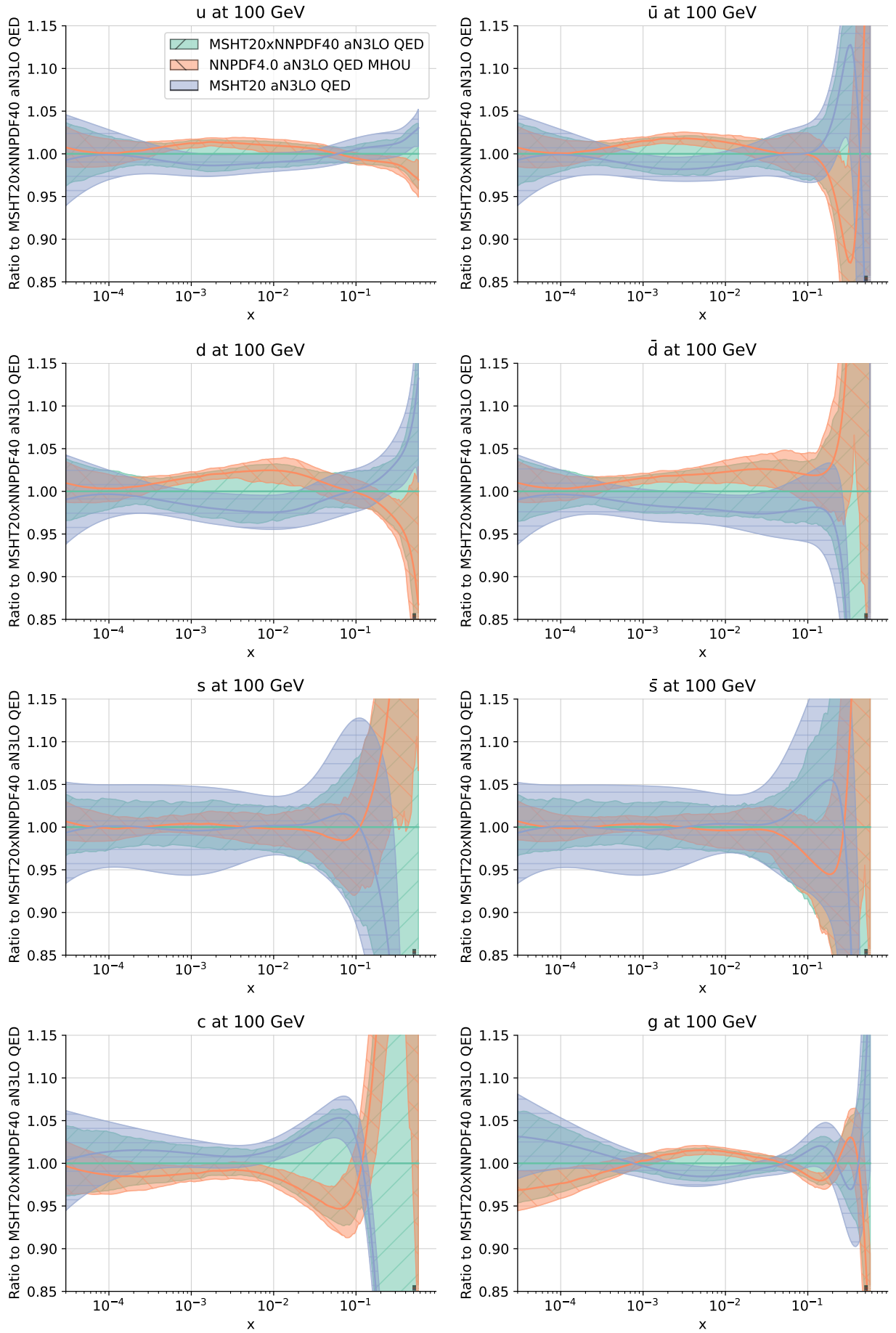


Figure 8. Same as Fig. 7, but for the QED PDF sets.

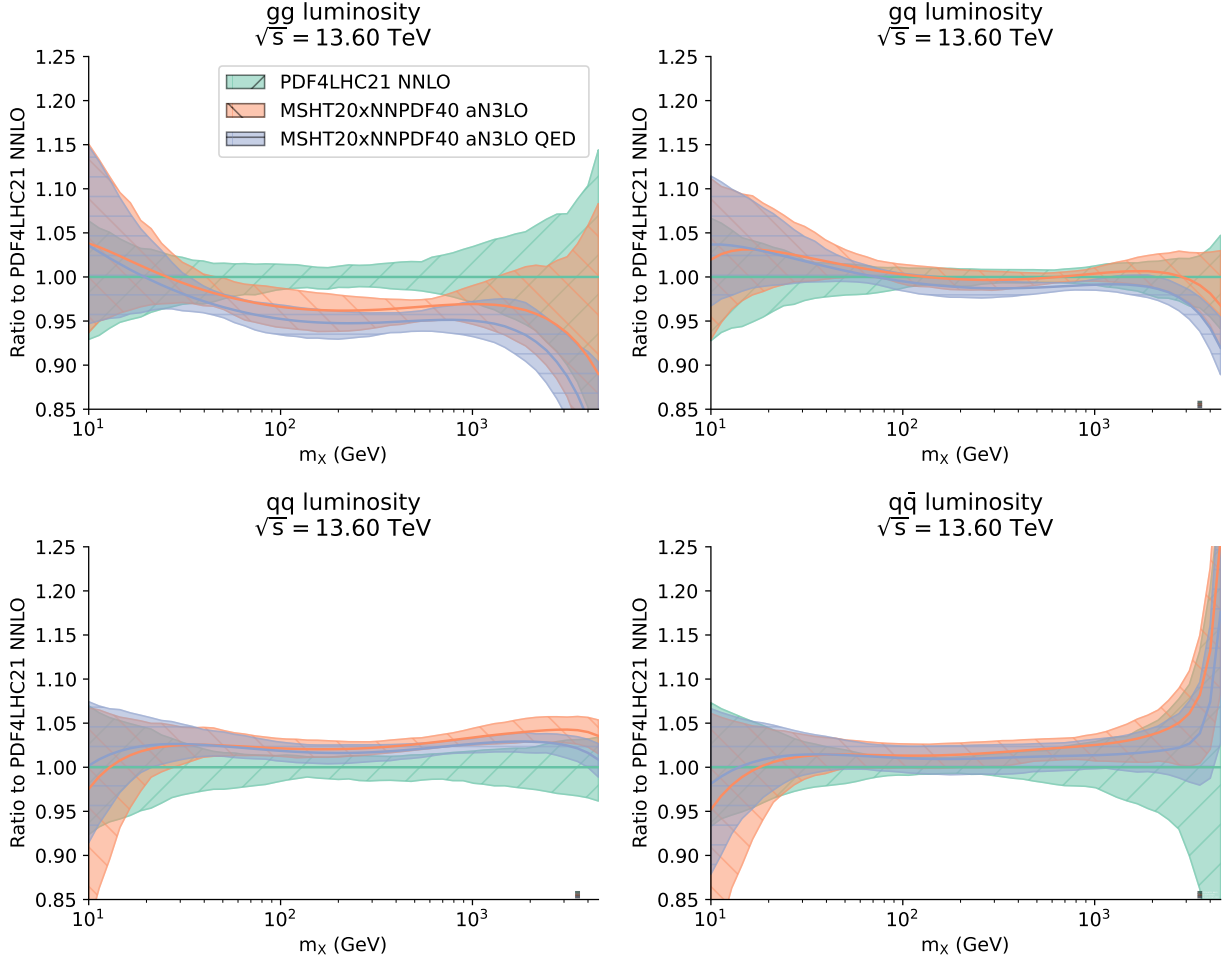


Figure 9. Parton luminosities for the LHC $\sqrt{s} = 13.6$ TeV computed from the MSHT20xNNPDF40_aN3LO pure QCD and QCD+QED sets, compared to the NNLO PDF4LHC21 result, and shown a ratio to the latter.

corrections. Results obtained by using perturbatively mismatched NNLO PDFs together with the N^3 LO matrix element are also shown, both for the PDF4LHC21 and MSHT20xNNPDF40 NNLO combined sets. In order to visually assess the error involved in this procedure, in Fig. 11 we also show results as a ratio of the result to that found using mismatched NNLO PDFs, specifically from the MSHT20xNNPDF40_NNLO combined baseline set.

The percentage error made when using mismatched NNLO PDFs is

$$\Delta_{\text{NNLO}}^{\text{exact}} \equiv \left| \frac{\sigma_{\text{N}^3\text{LO-PDF}}^{\text{N}^3\text{LO}} - \sigma_{\text{NNLO-PDF}}^{\text{N}^3\text{LO}}}{\sigma_{\text{N}^3\text{LO-PDF}}^{\text{N}^3\text{LO}}} \right|. \quad (1)$$

An approximate way of estimating this error before knowledge of a N^3 LO PDFs, based on the behavior seen at one less perturbative order, was suggested in Refs. [43, 44] and it is given by

$$\Delta_{\text{NNLO}}^{\text{app}} \equiv \frac{1}{2} \left| \frac{\sigma_{\text{NNLO-PDF}}^{\text{NNLO}} - \sigma_{\text{NLO-PDF}}^{\text{NNLO}}}{\sigma_{\text{NNLO-PDF}}^{\text{NNLO}}} \right|. \quad (2)$$

The values of $\Delta_{\text{NNLO}}^{\text{exact}}$ of $\Delta_{\text{NNLO}}^{\text{app}}$ obtained for each process are also included in Tables 1-2, both for NNPDF4.0, MSHT20, and the combined PDF sets constructed here, using in each case PDFs at the required perturbative orders from the same set. For the computation of $\Delta_{\text{NNLO}}^{\text{app}}$ for the combined set we use as a value for $\sigma_{\text{NLO-PDF}}^{\text{NNLO}}$ the average of the cross-sections computed using NNPDF4.0 and MSHT20 NLO PDFs.

It is clear that, as already noticed from the comparison of parton luminosities of Figs. 9-10, the effect of using a N^3 LO PDFs is most substantial for gluon fusion and vector boson fusion, which depend on the gluon-gluon and quark-quark luminosity respectively, and is small for associated hV production, which depends on the quark-antiquark luminosity. It follows that for gluon fusion and VBF using mismatched NNLO PDFs leads to a large error $\Delta_{\text{NNLO}}^{\text{exact}}$. Furthermore, the approximate estimate of this error $\Delta_{\text{NNLO}}^{\text{app}}$ is very unreliable,

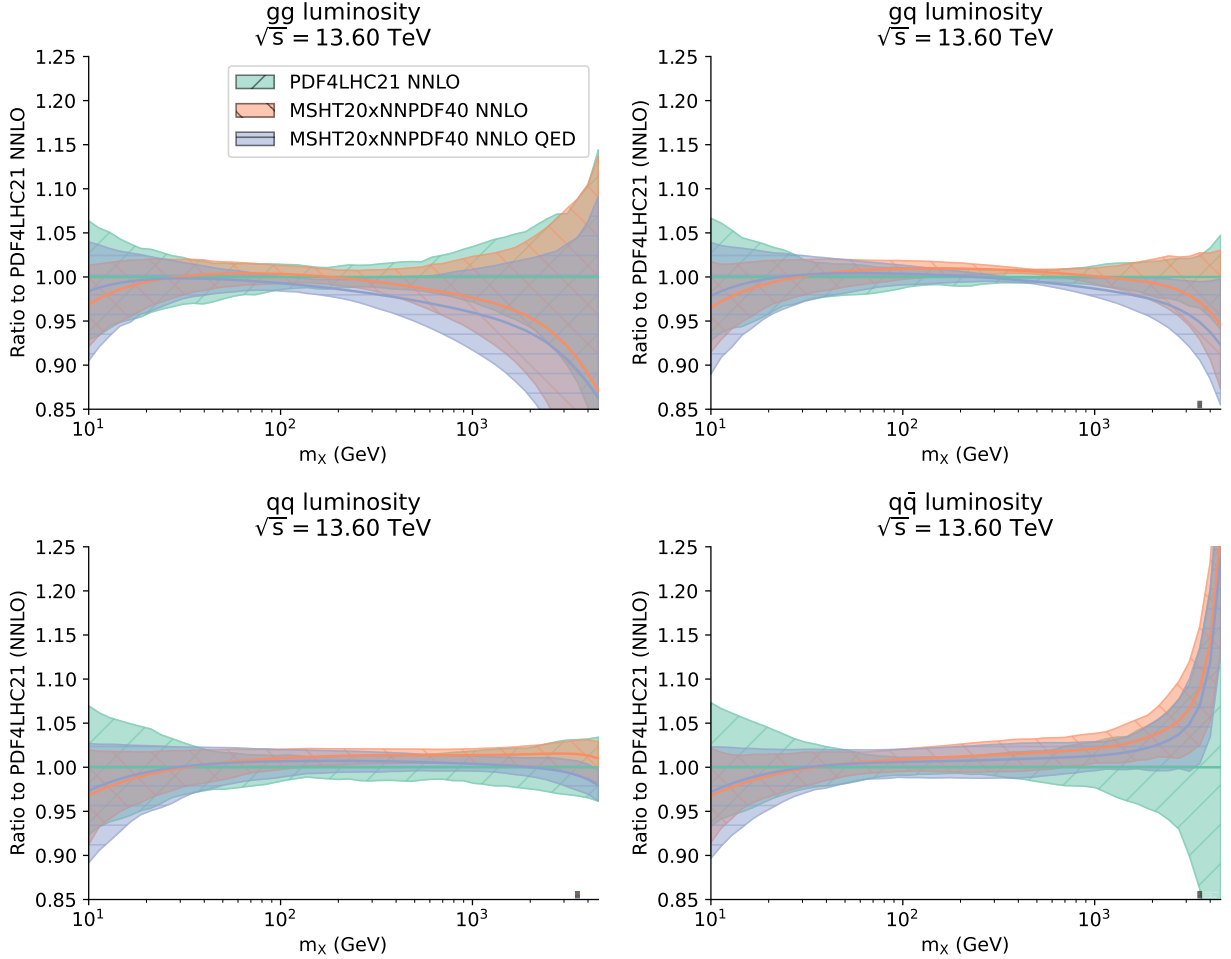


Figure 10. Comparison of NNLO parton luminosities for the LHC with $\sqrt{s} = 13.6$ TeV: the MSHT20xNNPDF40_nnlo pure QCD and QCD+QED results are compared to the PDF4LHC21 combination.

and specifically for gluon fusion and VBF it underestimates the true $\Delta_{\text{NNLO}}^{\text{exact}}$ significantly. The fact that for gluon fusion $\Delta_{\text{NNLO}}^{\text{app}}$ is rather smaller than $\Delta_{\text{NNLO}}^{\text{exact}}$ means that the difference between using N³LO and NNLO PDFs is significantly larger than one may expect comparing the change at the previous order, thus belying expectations [44, 56] that the impact of N³LO PDFs would be very small based on the behavior of the previous orders. This is a consequence of the behavior of the gluon luminosity discussed at the end of Sect. 3.

Indeed, for gluon fusion there is a compensation between the hard cross-section and the gluon PDF when both are used at N³LO, with the former leading to a significant increase which is then largely eliminated by the reduced gluon distribution in the correctly matched PDFs. For VBF, instead, the use of aN³LO PDFs leads to a clear increase of 2.5% compared to using NNLO PDFs in all cases, much larger than the fixed-order uncertainty.

The choice of a specific PDF (either of the individual sets or any of the combinations) entering the calculation has a relatively small effect on VBF, either at NNLO or aN³LO. For gluon fusion this choice has a negligible effect at NNLO, while at aN³LO, as repeatedly observed, a stronger suppression is found using MSHT20 than NNPDF4.0 PDFs, with the combination providing a value in between and an uncertainty encompassing the different degrees of suppression. Hence in both cases, the error made using NNLO PDFs is larger than the PDF uncertainties, and also larger than the spread of aN³LO results. The picture is somewhat different for associate Higgs production. For this process, the impact of using aN³LO vs. NNLO PDFs is negligible, so the dominant difference comes from the choice of PDF set, though results found using any of the PDF sets or combinations considered here all agree within uncertainties.

Finally, we observe that for Higgs production in gluon fusion the effect of QED corrections, again as already seen in luminosities, is also not negligible, though smaller than that of using properly matched PDFs.

It is finally interesting to compare results obtained using the MC combination of aN³LO PDF sets to those that would be found by performing the textbook weighted average and uncertainty. For gluon fusion

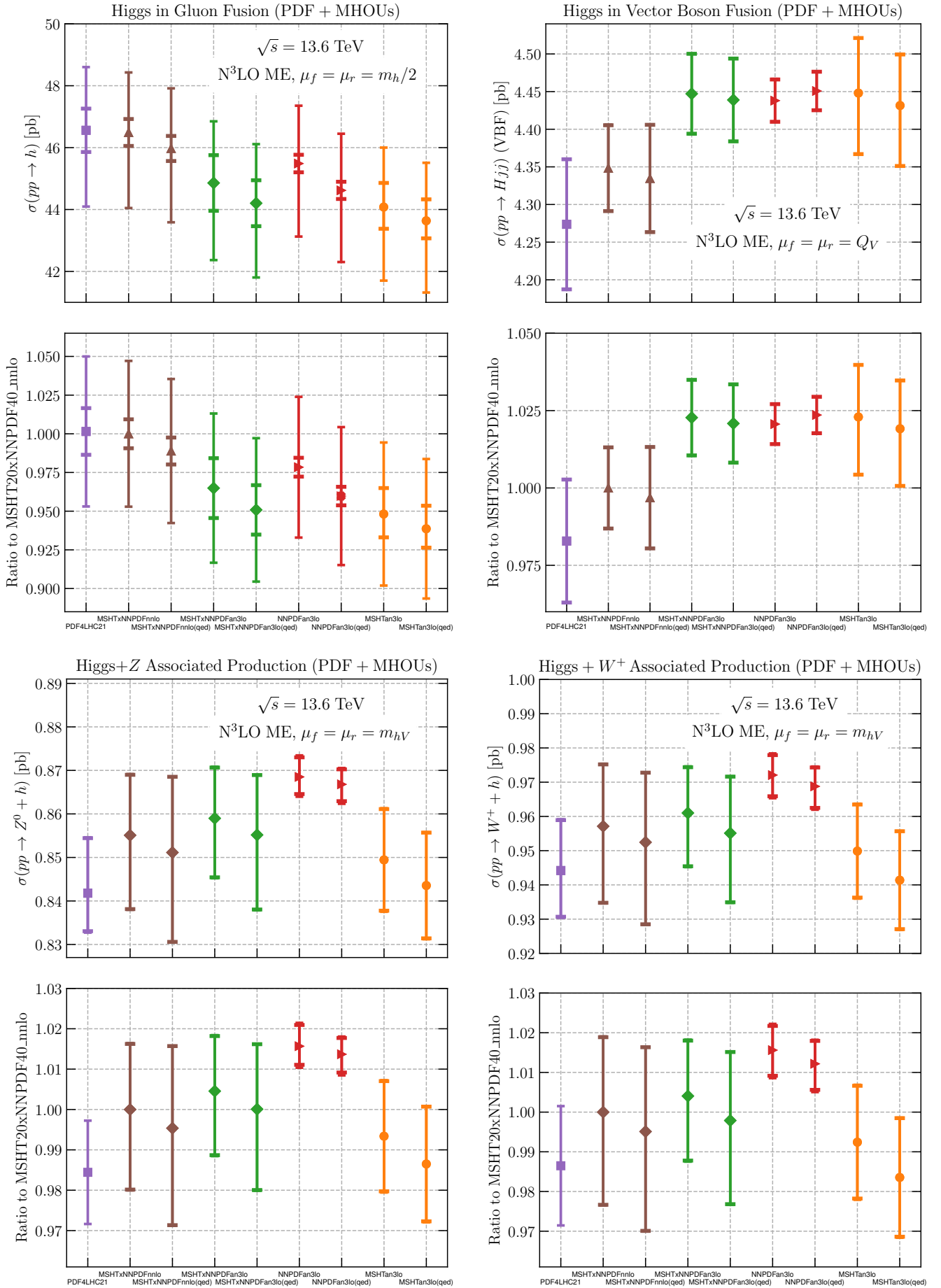


Figure 11. The cross-sections of Tables 1-2, shown both in absolute scale (top) or as ratios to the result found using the MSHT20xNNPDF40_nnlo baseline combination. In all cases, N³LO matrix elements are used. The results for hW^- are qualitatively similar as those for hW^+ and not shown. The inner interval is the pure PDF uncertainty (first uncertainty in Tables 1-2) while the outer interval is the sum in quadrature of the PDF uncertainty and the MHOUs uncertainty on the hard cross section (second uncertainty in Tables 1-2).

PDF set	pert. order (PDF)	$\sigma(gg \rightarrow h)$	$\sigma(h \text{ VBF})$
PDF4LHC21_mc	NNLO _{QCD}	46.56 ^{+1.5%} _{-1.5%} ^{+4.4%} _{-5.3%}	4.27 ^{+2.0%} _{-2.0%} ^{+2.0%} _{-2.0%}
MSHT20xNNPDF40_nnlo	NNLO _{QCD}	46.49 ^{+0.9%} _{-0.9%} ^{+4.2%} _{-5.3%}	4.35 ^{+1.3%} _{-1.3%} ^{+1.3%} _{-1.3%}
MSHT20xNNPDF40_nnlo_qed	NNLO _{QCD} \otimes NLO _{QED}	45.97 ^{+0.9%} _{-0.9%} ^{+4.3%} _{-5.4%}	4.34 ^{+1.6%} _{-1.6%} ^{+1.6%} _{-1.6%}
MSHT20xNNPDF40_an3lo	aN ³ LO _{QCD}	44.86 ^{+2.0%} _{-2.0%} ^{+4.4%} _{-5.6%}	4.45 ^{+1.2%} _{-1.2%} ^{+1.2%} _{-1.2%}
MSHT20xNNPDF40_an3lo_qed	aN ³ LO _{QCD} \otimes NLO _{QED}	44.20 ^{+1.7%} _{-1.7%} ^{+4.3%} _{-5.4%}	4.44 ^{+1.2%} _{-1.2%} ^{+1.2%} _{-1.2%}
NNPDF40_an3lo_as.01180_mhou	aN ³ LO _{QCD}	45.49 ^{+0.6%} _{-0.6%} ^{+4.1%} _{-5.2%}	4.44 ^{+0.6%} _{-0.6%} ^{+0.7%} _{-0.6%}
NNPDF40_an3lo_as.01180_qed_mhou	aN ³ LO _{QCD} \otimes NLO _{QED}	44.62 ^{+0.6%} _{-0.6%} ^{+4.1%} _{-5.2%}	4.45 ^{+0.6%} _{-0.6%} ^{+0.6%} _{-0.6%}
MSHT20an3lo_as118	aN ³ LO _{QCD}	44.08 ^{+1.8%} _{-1.6%} ^{+4.4%} _{-5.6%}	4.44 ^{+1.6%} _{-1.8%} ^{+1.7%} _{-1.8%}
MSHT20qed_an3lo	aN ³ LO _{QCD} \otimes NLO _{QED}	43.63 ^{+1.6%} _{-1.3%} ^{+4.3%} _{-5.3%}	4.43 ^{+1.5%} _{-1.8%} ^{+1.5%} _{-1.8%}
$\Delta_{\text{NNLO}}^{\text{exact}}$ (NNPDF4.0)		2.2%	1.3%
$\Delta_{\text{NNLO}}^{\text{exact}}$ (MSHT20)		5.3%	2.3%
$\Delta_{\text{NNLO}}^{\text{exact}}$ (combination)		3.3%	2.3%
$\Delta_{\text{NNLO}}^{\text{app}}$ (NNPDF4.0)		0.2%	0.2%
$\Delta_{\text{NNLO}}^{\text{app}}$ (MSHT20)		1.4%	1.3%
$\Delta_{\text{NNLO}}^{\text{app}}$ (combination)		0.9%	0.5%

Table 1. The total inclusive cross-section (in pb) for Higgs production in gluon-fusion and in associated production at the LHC Run 3 with $\sqrt{s} = 13.6$ TeV. In all cases, the partonic matrix element is evaluated at N³LO accuracy not including QED or electroweak corrections. The central scales are set to be $\mu_{F,R} = m_h/2$ (gluon fusion) and $\mu_{F,R} = Q_V$ (VBF). The first uncertainty shown is the pure PDF uncertainty, and the second is the sum in quadrature of the PDF uncertainty and the MHOU on the hard cross-section evaluated with the 7-point prescription. The PDF4LHC21_mc and MSHT20xNNPDF40_nnlo PDF sets are at NNLO, while all the other PDF sets are determined at aN³LO accuracy. The error $\Delta_{\text{NNLO}}^{\text{exact}}$, Eq. (1), that is made when using NNLO PDFs with the aN³LO matrix element, and its approximate estimate $\Delta_{\text{NNLO}}^{\text{app}}$, Eq. (2), are also provided both separately for NNPDF4.0, MSHT20, and for their combination in the case of the pure QCD fits.

the weighted combination (with weights $1/\delta_{\text{pdf}}^2$) gives

$$\sigma_{\text{ggF}}^{\text{comb}} = 45.30 \pm 0.28_{\text{pdf}} \text{ pb} \quad (\text{pure QCD}) \quad (3)$$

$$\sigma_{\text{ggF}}^{\text{comb}} = 44.43 \pm 0.26_{\text{pdf}} \text{ pb} \quad (\text{QCD+QED}). \quad (4)$$

This is to be compared with the result found using the MSHT20xNNPDF40 aN³LO sets (both pure QCD and QCD \otimes QED) from Table 1, namely

$$\sigma_{\text{ggF}}^{\text{MSHTxNNPDF}} = 44.86 \pm 0.90_{\text{pdf}} \text{ pb} \quad (\text{pure QCD}) \quad (5)$$

$$\sigma_{\text{ggF}}^{\text{MSHTxNNPDF-qed}} = 44.20 \pm 0.75_{\text{pdf}} \text{ pb} \quad (\text{QCD+QED}). \quad (6)$$

where in both cases we consider only the PDF uncertainty. It is clear that the latter result is significantly more conservative, in that it treats the two existing sets on the same footing and leads to a correspondingly rather larger uncertainty. Eqs. (5)–(6) should be considered our best result for Higgs production in gluon

PDF set	pert. order (PDF)	$\sigma(hW^+)$	$\sigma(hW^-)$	$\sigma(hZ)$
PDF4LHC21_mc	NNLO _{QCD}	0.944 ^{+1.6%} _{-1.4%} ^{+1.6%} _{-1.5%}	0.593 ^{+1.5%} _{-1.2%} ^{+1.5%} _{-1.3%}	0.842 ^{+1.5%} _{-1.0%} ^{+1.5%} _{-1.1%}
MSHT20xNNPDF40_nnlo	NNLO _{QCD}	0.957 ^{+1.9%} _{-2.3%} ^{+1.9%} _{-2.4%}	0.601 ^{+1.5%} _{-2.2%} ^{+1.6%} _{-2.2%}	0.855 ^{+1.6%} _{-2.0%} ^{+1.6%} _{-2.0%}
MSHT20xNNPDF40_nnlo_qed	NNLO _{QCD} \otimes NLO _{QED}	0.952 ^{+2.1%} _{-2.5%} ^{+2.1%} _{-2.5%}	0.598 ^{+1.8%} _{-2.5%} ^{+1.8%} _{-2.5%}	0.851 ^{+2.0%} _{-2.4%} ^{+2.1%} _{-2.4%}
MSHT20xNNPDF40_an3lo	aN ³ LO _{QCD}	0.961 ^{+1.4%} _{-1.6%} ^{+1.4%} _{-1.6%}	0.604 ^{+1.2%} _{-1.6%} ^{+1.2%} _{-1.6%}	0.859 ^{+1.4%} _{-1.6%} ^{+1.4%} _{-1.6%}
MSHT20xNNPDF40_an3lo_qed	aN ³ LO _{QCD} \otimes NLO _{QED}	0.955 ^{+1.7%} _{-2.1%} ^{+1.7%} _{-2.1%}	0.601 ^{+1.4%} _{-2.0%} ^{+1.4%} _{-2.0%}	0.855 ^{+1.6%} _{-2.0%} ^{+1.6%} _{-2.0%}
NNPDF40_an3lo_as_01180_mhou	aN ³ LO _{QCD}	0.972 ^{+0.6%} _{-0.6%} ^{+0.7%} _{-0.7%}	0.610 ^{+0.6%} _{-0.6%} ^{+0.6%} _{-0.7%}	0.869 ^{+0.5%} _{-0.5%} ^{+0.6%} _{-0.5%}
NNPDF40_an3lo_as_01180_qed_mhou	aN ³ LO _{QCD} \otimes NLO _{QED}	0.969 ^{+0.6%} _{-0.6%} ^{+0.6%} _{-0.7%}	0.608 ^{+0.5%} _{-0.6%} ^{+0.6%} _{-0.7%}	0.867 ^{+0.4%} _{-0.4%} ^{+0.4%} _{-0.5%}
MSHT20an3lo_as118	aN ³ LO _{QCD}	0.950 ^{+1.4%} _{-1.4%} ^{+1.5%} _{-1.5%}	0.599 ^{+1.5%} _{-1.5%} ^{+1.5%} _{-1.5%}	0.849 ^{+1.4%} _{-1.4%} ^{+1.4%} _{-1.4%}
MSHT20qed_an3lo	aN ³ LO _{QCD} \otimes NLO _{QED}	0.941 ^{+1.5%} _{-1.5%} ^{+1.5%} _{-1.5%}	0.595 ^{+1.6%} _{-1.6%} ^{+1.6%} _{-1.6%}	0.844 ^{+1.4%} _{-1.4%} ^{+1.5%} _{-1.5%}
$\Delta_{\text{NNLO}}^{\text{exact}}$ (NNPDF4.0)		0.5%	0.3%	0.3%
$\Delta_{\text{NNLO}}^{\text{exact}}$ (MSHT20)		0.9%	1.0%	0.8%
$\Delta_{\text{NNLO}}^{\text{exact}}$ (combination)		0.6%	0.5%	0.5%
$\Delta_{\text{NNLO}}^{\text{app}}$ (NNPDF4.0)		0.2%	0.2%	0.1%
$\Delta_{\text{NNLO}}^{\text{app}}$ (MSHT20)		0.8%	0.9%	1.1%
$\Delta_{\text{NNLO}}^{\text{app}}$ (combination)		0.1%	0.2%	0.3%

Table 2. Same as Table 1 for Higgs production in association with vector bosons.

fusion, although we emphasize that the difference between this and the weighted average remains lower than the difference between the predictions based on NNLO and aN³LO PDFs.

5 Conclusion

In this note we have shown that the use of aN³LO PDFs is mandatory for accurate N³LO phenomenology at the LHC, focusing on the case of Higgs production cross-sections. For Higgs production in gluon fusion and in vector boson fusion the impact of switching from NNLO to aN³LO PDFs is rather larger than the PDF uncertainty, and also larger (for VBF much larger) than the difference between different PDF sets. Indeed, we have shown that differences between existing aN³LO PDF sets are moderate, and generally smaller than the difference between NNLO and aN³LO.

Our results illustrate the limitations of N³LO phenomenology at the LHC using NNLO PDFs. In order to deal with these limitations, we have constructed combined aN³LO PDF sets, both pure QCD and QCD+QED, which allow for the computation of phenomenological predictions with a more conservative estimate of the uncertainty, as is appropriate when combining predictions that are not fully compatible. Clearly, a full N³LO PDF determination will only be possible once all processes currently used for PDF determination are known at this order, which is likely to take some time. In particular, the calculation of the massive corrections to the DIS coefficient functions and the full set of N³LO corrections to hadronic processes will almost certainly take many years to compute. In the meantime, our results clearly demonstrate that the available aN³LO PDFs represent the most accurate option for the deployment of N³LO calculations for LHC physics.

The MSHT20xNNPDF40_an3lo and MSHT20xNNPDF40_an3lo_qed PDF sets presented in this note have been submitted to the LHAPDF repository [57]. They are also made available (alongside the corresponding NNLO baseline sets) at the link:

<https://zenodo.org/records/13843626>.

Acknowledgments

We thank the convenors of Working Group 1 of the LHC Higgs Cross-Section Working Group (LHCHXSWG), in particular the gluon-fusion subgroup, for constructive feedback on the first draft of this document. We are also grateful to Amanda Cooper-Sarkar for questions and critical input, and members of the CT collaboration, in particular Joey Huston and Pavel Nadolsky, for discussion concerning N^3 LO PDFs and their uncertainties.

S. F. performed this work in part at the Aspen Center for Physics, which is supported by National Science Foundation Grant PHY-2210452, and is partially supported by an Italian PRIN2022 grant. R. D. B., L. D. D. and R. S. thank STFC for support via grant awards ST/T000600/1 and ST/X000494/1. L. H.-L. and R. S. T. thank STFC for support via grant awards ST/T000856/1 and ST/X000516/1. T. C. acknowledges that this project has received funding from the European Research Council (ERC) under the European Union’s Horizon 2020 research and innovation programme (Grant agreement No. 101002090 COLORFREE). E. R. N. is supported by the Italian Ministry of University and Research (MUR) through the “Rita Levi-Montalcini” Program. F. H. is supported by the Academy of Finland project 358090 and is funded as a part of the Center of Excellence in Quark Matter of the Academy of Finland, project 346326. M.U. is supported by the European Research Council under the European Union’s Horizon 2020 research and innovation Programme (grant agreement n.950246), and partially by the STFC consolidated grant ST/T000694/1 and ST/X000664/1.

References

- [1] S. Bailey, T. Cridge, L. A. Harland-Lang, A. D. Martin, and R. S. Thorne, *Parton distributions from LHC, HERA, Tevatron and fixed target data: MSHT20 PDFs*, *Eur. Phys. J. C* **81** (2021), no. 4 341, [[arXiv:2012.04684](#)].
- [2] NNPDF Collaboration, R. D. Ball et al., *The path to proton structure at 1% accuracy*, *Eur. Phys. J. C* **82** (2022), no. 5 428, [[arXiv:2109.02653](#)].
- [3] J. McGowan, T. Cridge, L. A. Harland-Lang, and R. S. Thorne, *Approximate N^3 LO parton distribution functions with theoretical uncertainties: MSHT20a N^3 LO PDFs*, *Eur. Phys. J. C* **83** (2023), no. 3 185, [[arXiv:2207.04739](#)]. [Erratum: *Eur.Phys.J.C* 83, 302 (2023)].
- [4] NNPDF Collaboration, R. D. Ball et al., *The path to N^3 LO parton distributions*, *Eur. Phys. J. C* **84** (2024), no. 7 659, [[arXiv:2402.18635](#)].
- [5] T. Cridge, L. A. Harland-Lang, and R. S. Thorne, *Combining QED and approximate N^3 LO QCD corrections in a global PDF fit: MSHT20qed_an3lo PDFs*, *SciPost Phys.* **17** (2024), no. 1 026, [[arXiv:2312.07665](#)].
- [6] A. Barontini, N. Laurenti, and J. Rojo, *NNPDF4.0 a N^3 LO PDFs with QED corrections*, in *31st International Workshop on Deep-Inelastic Scattering and Related Subjects*, 6, 2024. [[arXiv:2406.01779](#)].
- [7] S. Moch, B. Ruijl, T. Ueda, J. A. M. Vermaseren, and A. Vogt, *Four-Loop Non-Singlet Splitting Functions in the Planar Limit and Beyond*, *JHEP* **10** (2017) 041, [[arXiv:1707.08315](#)].
- [8] J. Davies, A. Vogt, B. Ruijl, T. Ueda, and J. A. M. Vermaseren, *Large- n_f contributions to the four-loop splitting functions in QCD*, *Nucl. Phys. B* **915** (2017) 335–362, [[arXiv:1610.07477](#)].
- [9] T. Gehrmann, A. von Manteuffel, V. Sotnikov, and T.-Z. Yang, *Complete N_f^2 contributions to four-loop pure-singlet splitting functions*, *JHEP* **01** (2024) 029, [[arXiv:2308.07958](#)].

- [10] T. Gehrmann, A. von Manteuffel, V. Sotnikov, and T.-Z. Yang, *The $N_f C_F^3$ contribution to the non-singlet splitting function at four-loop order*, *Phys. Lett. B* **849** (2024) 138427, [[arXiv:2310.12240](#)].
- [11] G. Falcioni, F. Herzog, S. Moch, J. Vermaseren, and A. Vogt, *The double fermionic contribution to the four-loop quark-to-gluon splitting function*, *Phys. Lett. B* **848** (2024) 138351, [[arXiv:2310.01245](#)].
- [12] S. Moch, B. Ruijl, T. Ueda, J. A. M. Vermaseren, and A. Vogt, *On quartic colour factors in splitting functions and the gluon cusp anomalous dimension*, *Phys. Lett. B* **782** (2018) 627–632, [[arXiv:1805.09638](#)].
- [13] S. Moch, B. Ruijl, T. Ueda, J. A. M. Vermaseren, and A. Vogt, *Low moments of the four-loop splitting functions in QCD*, *Phys. Lett. B* **825** (2022) 136853, [[arXiv:2111.15561](#)].
- [14] G. Falcioni, F. Herzog, S. Moch, and A. Vogt, *Four-loop splitting functions in QCD – The quark-quark case*, *Phys. Lett. B* **842** (2023) 137944, [[arXiv:2302.07593](#)].
- [15] G. Falcioni, F. Herzog, S. Moch, and A. Vogt, *Four-loop splitting functions in QCD – The gluon-to-quark case*, *Phys. Lett. B* **846** (2023) 138215, [[arXiv:2307.04158](#)].
- [16] S. Moch, B. Ruijl, T. Ueda, J. Vermaseren, and A. Vogt, *Additional moments and x -space approximations of four-loop splitting functions in QCD*, *Phys. Lett. B* **849** (2024) 138468, [[arXiv:2310.05744](#)].
- [17] G. Falcioni, F. Herzog, S. Moch, A. Pelloni, and A. Vogt, *Four-loop splitting functions in QCD – The quark-to-gluon case*, *Phys. Lett. B* **856** (2024) 138906, [[arXiv:2404.09701](#)].
- [18] G. Falcioni, F. Herzog, S. Moch, and S. Van Thurenhout, *Constraints for twist-two alien operators in QCD*, [[arXiv:2409.02870](#)].
- [19] G. Falcioni, F. Herzog, S. Moch, A. Pelloni, and A. Vogt, *Four-loop splitting functions in QCD – The gluon-gluon case –*, [[arXiv:2410.08089](#)].
- [20] H. Kawamura, N. A. Lo Presti, S. Moch, and A. Vogt, *On the next-to-next-to-leading order QCD corrections to heavy-quark production in deep-inelastic scattering*, *Nucl. Phys. B* **864** (2012) 399–468, [[arXiv:1205.5727](#)].
- [21] I. Bierenbaum, J. Blümlein, and S. Klein, *Mellin Moments of the $O(\alpha_s^3)$ Heavy Flavor Contributions to unpolarized Deep-Inelastic Scattering at $Q^2 \gg m^2$ and Anomalous Dimensions*, *Nucl. Phys. B* **820** (2009) 417–482, [[arXiv:0904.3563](#)].
- [22] J. Ablinger, A. Behring, J. Blümlein, A. De Freitas, A. Hasselhuhn, A. von Manteuffel, M. Round, C. Schneider, and F. Wißbrock, *The 3-Loop Non-Singlet Heavy Flavor Contributions and Anomalous Dimensions for the Structure Function $F_2(x, Q^2)$ and Transversity*, *Nucl. Phys. B* **886** (2014) 733–823, [[arXiv:1406.4654](#)].
- [23] J. Ablinger, A. Behring, J. Blümlein, A. De Freitas, A. von Manteuffel, and C. Schneider, *The 3-loop pure singlet heavy flavor contributions to the structure function $F_2(x, Q^2)$ and the anomalous dimension*, *Nucl. Phys. B* **890** (2014) 48–151, [[arXiv:1409.1135](#)].
- [24] J. Blümlein, P. Marquard, C. Schneider, and K. Schönwald, *The three-loop unpolarized and polarized non-singlet anomalous dimensions from off shell operator matrix elements*, *Nucl. Phys. B* **971** (2021) 115542, [[arXiv:2107.06267](#)].
- [25] J. Ablinger, J. Blümlein, A. De Freitas, A. Hasselhuhn, A. von Manteuffel, M. Round, and C. Schneider, *The $O(\alpha_s^3 T_F^2)$ Contributions to the Gluonic Operator Matrix Element*, *Nucl. Phys. B* **885** (2014) 280–317, [[arXiv:1405.4259](#)].
- [26] J. Ablinger, J. Blümlein, A. De Freitas, A. Hasselhuhn, A. von Manteuffel, M. Round, and C. Schneider, *3-loop Massive $O(T_F^2)$ Contributions to the DIS Operator Matrix Element A_{gg}* , *Nucl. Part. Phys. Proc.* **258-259** (2015) 37–40, [[arXiv:1409.1435](#)].

- [27] J. Ablinger, J. Blümlein, A. De Freitas, A. Hasselhuhn, A. von Manteuffel, M. Round, C. Schneider, and F. Wißbrock, *The transition matrix element $A_{gg}(N)$ of the variable flavor number scheme at $O(\alpha_s^3)$* , *Nuclear Physics B* **882** (May, 2014) 263–288, [[arXiv:1402.0359](#)].
- [28] J. Ablinger, A. Behring, J. Blümlein, A. De Freitas, A. Goedicke, A. von Manteuffel, C. Schneider, and K. Schönwald, *The unpolarized and polarized single-mass three-loop heavy flavor operator matrix elements $A_{gg,Q}$ and $\Delta A_{gg,Q}$* , *JHEP* **12** (2022) 134, [[arXiv:2211.05462](#)].
- [29] J. Ablinger, A. Behring, J. Blümlein, A. De Freitas, A. von Manteuffel, C. Schneider, and K. Schönwald, *The first-order factorizable contributions to the three-loop massive operator matrix elements $A_{Qg}(3)$ and $\Delta A_{Qg}(3)$* , *Nucl. Phys. B* **999** (2024) 116427, [[arXiv:2311.00644](#)].
- [30] J. Ablinger, A. Behring, J. Blümlein, A. De Freitas, A. von Manteuffel, C. Schneider, and K. Schönwald, *The non-first-order-factorizable contributions to the three-loop single-mass operator matrix elements $A_{Qg}^{(3)}$ and $\Delta A_{Qg}^{(3)}$* , [arXiv:2403.00513](#).
- [31] J. A. M. Vermaseren, A. Vogt, and S. Moch, *The third-order QCD corrections to deep-inelastic scattering by photon exchange*, *Nucl. Phys.* **B724** (2005) 3, [[hep-ph/0504242](#)].
- [32] F. Caola, W. Chen, C. Duhr, X. Liu, B. Mistlberger, F. Petriello, G. Vita, and S. Weinzierl, *The Path forward to N^3LO* , in *Snowmass 2021*, 3, 2022. [arXiv:2203.06730](#).
- [33] C. Duhr, F. Dulat, and B. Mistlberger, *Charged current Drell-Yan production at N^3LO* , *JHEP* **11** (2020) 143, [[arXiv:2007.13313](#)].
- [34] C. Duhr, F. Dulat, and B. Mistlberger, *Drell-Yan Cross Section to Third Order in the Strong Coupling Constant*, *Phys. Rev. Lett.* **125** (2020), no. 17 172001, [[arXiv:2001.07717](#)].
- [35] C. Duhr and B. Mistlberger, *Lepton-pair production at hadron colliders at N^3LO in QCD*, *JHEP* **03** (2022) 116, [[arXiv:2111.10379](#)].
- [36] X. Chen, T. Gehrmann, N. Glover, A. Huss, T.-Z. Yang, and H. X. Zhu, *Dilepton Rapidity Distribution in Drell-Yan Production to Third Order in QCD*, *Phys. Rev. Lett.* **128** (2022), no. 5 052001, [[arXiv:2107.09085](#)].
- [37] R. D. Ball, S. Carrazza, L. Del Debbio, S. Forte, J. Gao, et al., *Parton Distribution Benchmarking with LHC Data*, *JHEP* **1304** (2013) 125, [[arXiv:1211.5142](#)].
- [38] R. D. Ball and R. L. Pearson, *Correlation of theoretical uncertainties in PDF fits and theoretical uncertainties in predictions*, *Eur. Phys. J. C* **81** (2021), no. 9 830, [[arXiv:2105.05114](#)].
- [39] J. Davies, C. H. Kom, S. Moch, and A. Vogt, *Resummation of small- x double logarithms in QCD: inclusive deep-inelastic scattering*, *JHEP* **08** (2022) 135, [[arXiv:2202.10362](#)].
- [40] J. Andersen et al., *Les Houches 2023: Physics at TeV Colliders: Standard Model Working Group Report*, in *Physics of the TeV Scale and Beyond the Standard Model: Intensifying the Quest for New Physics*, 6, 2024. [arXiv:2406.00708](#).
- [41] A. Cooper-Sarkar, T. Cridge, F. Giuli, L. A. Harland-Lang, F. Hekhorn, J. Huston, G. Magni, S. Moch, and R. S. Thorne, *A Benchmarking of QCD Evolution at Approximate N^3LO* , [arXiv:2406.16188](#).
- [42] R. S. Thorne, T. Cridge, and L. Harland-Lang, *MSHT Updates 2024*, in *31st International Workshop on Deep-Inelastic Scattering and Related Subjects*, 8, 2024. [arXiv:2408.10008](#).
- [43] J. Baglio, C. Duhr, B. Mistlberger, and R. Szafron, *Inclusive production cross sections at N^3LO* , *JHEP* **12** (2022) 066, [[arXiv:2209.06138](#)].
- [44] C. Anastasiou, C. Duhr, F. Dulat, E. Furlan, T. Gehrmann, F. Herzog, A. Lazopoulos, and B. Mistlberger, *High precision determination of the gluon fusion Higgs boson cross-section at the LHC*, *JHEP* **05** (2016) 058, [[arXiv:1602.00695](#)].

- [45] J. Butterworth et al., *PDF4LHC recommendations for LHC Run II*, *J. Phys.* **G43** (2016) 023001, [[arXiv:1510.03865](#)].
- [46] **NNPDF** Collaboration, R. D. Ball et al., *Determination of the theory uncertainties from missing higher orders on NNLO parton distributions with percent accuracy*, *Eur. Phys. J. C* **84** (2024), no. 5 517, [[arXiv:2401.10319](#)].
- [47] **PDF4LHC Working Group** Collaboration, R. D. Ball et al., *The PDF4LHC21 combination of global PDF fits for the LHC Run III*, *J. Phys. G* **49** (2022), no. 8 080501, [[arXiv:2203.05506](#)].
- [48] **PDF4LHC21 combination group** Collaboration, T. Cridge, *PDF4LHC21: Update on the benchmarking of the CT, MSHT and NNPDF global PDF fits*, *SciPost Phys. Proc.* **8** (2022) 101, [[arXiv:2108.09099](#)].
- [49] J. Erler and R. Ferro-Hernández, *Alternative to the application of PDG scale factors*, *Eur. Phys. J. C* **80** (2020), no. 6 541, [[arXiv:2004.01219](#)].
- [50] **LHC Higgs Cross Section Working Group** Collaboration, S. Dittmaier et al., *Handbook of LHC Higgs Cross Sections: 1. Inclusive Observables*, [arXiv:1101.0593](#).
- [51] S. Carrazza, J. I. Latorre, J. Rojo, and G. Watt, *A compression algorithm for the combination of PDF sets*, *Eur. Phys. J.* **C75** (2015) 474, [[arXiv:1504.06469](#)].
- [52] G. Watt and R. S. Thorne, *Study of Monte Carlo approach to experimental uncertainty propagation with MSTW 2008 PDFs*, *JHEP* **1208** (2012) 052, [[arXiv:1205.4024](#)].
- [53] A. Manohar, P. Nason, G. P. Salam, and G. Zanderighi, *How bright is the proton? A precise determination of the photon parton distribution function*, *Phys. Rev. Lett.* **117** (2016), no. 24 242002, [[arXiv:1607.04266](#)].
- [54] F. A. Dreyer and A. Karlberg, *Vector-Boson Fusion Higgs Production at Three Loops in QCD*, *Phys. Rev. Lett.* **117** (2016), no. 7 072001, [[arXiv:1606.00840](#)].
- [55] F. A. Dreyer and A. Karlberg, *Vector-Boson Fusion Higgs Pair Production at N^3LO* , *Phys. Rev. D* **98** (2018), no. 11 114016, [[arXiv:1811.07906](#)].
- [56] S. Forte, A. Isgro, and G. Vita, *Do we need N^3LO Parton Distributions?*, *Phys.Lett.* **B731** (2014) 136–140, [[arXiv:1312.6688](#)].
- [57] A. Buckley, J. Ferrando, S. Lloyd, K. Nordström, B. Page, et al., *LHAPDF6: parton density access in the LHC precision era*, *Eur.Phys.J.* **C75** (2015) 132, [[arXiv:1412.7420](#)].